Reduction of the wave packet: Preferred observable and decoherence time scale

Juan Pablo Paz,* Salman Habib,† and Wojciech H. Zurek‡
Theoretical Astrophysics, T-6, Mail Stop B288, Los Alamos National Laboratory, Los Alamos, New Mexico 87545
(Received 28 May 1992)

Environment-induced destruction of quantum coherence is investigated in a simple model where the system is a harmonic oscillator, the environment is a collection of harmonic oscillators, and the interaction between them is linear in the position coordinate of the system. We study decoherence for initial states consisting of coherent superpositions of two Gaussian wave packets in either position or momentum. A new measure of the effectiveness of decoherence appropriate to the model and choice of initial conditions is proposed. By studying the dependence of the decoherence rate on the location of the initial peaks of the Wigner function, we clarify the sense in which position is a preferred observable even though position eigenstates are not the pointer states of this model. We analyze decoherence in the low-temperature regime and show that the usual "high-temperature" approximation is remarkably accurate in its domain of applicability. We also examine the relationship between the decoherence process and the frequency distribution of the environment oscillators (in particular, we focus attention on a specific "supra-Ohmic" environment). Implications of our results for the quantum to classical transition in various contexts are briefly explored.

PACS number(s): 03.65.Bz, 04.60.+n, 98.80.Dr

I. INTRODUCTION

The role of the interaction between a quantum system and its environment in the transition from the underlying quantum laws, based on the principle of superposition, to the familiar classical reality, where this principle appears to be violated, has been a subject of increasing interest, especially within the past decade. This surge of activity has been motivated by increasingly sophisticated experiments which allow one to probe the boundary between the quantum and classical as never before [1–3]. Furthermore, the interest in the transition from quantum to classical has also been boosted by the emergence of new contexts where a careful analysis of the reduction of the wave packet is of either fundamental (as in quantum cosmology [4]) or practical interest (as for detection of weak forces [5] or quantum optics [6]), and the traditional "Copenhagen interpretation" does not suffice. The key idea focuses on the process of *decoherence* by which quantum coherence is dynamically suppressed by the continuous buildup of nonseparable quantum correlations between the quantum system and the environment (see Ref. [7] for an introduction and a list of basic references and Refs. [8–11] for more detailed discussions). The outcome of such an interaction is the quick demise of the superpositions of states of the system that can be distinguished through their effect on the environment. This results in a negative selection which leads to the emergence of a preferred set of states, sometimes referred to as the "pointer basis" [8], which remain least affected by the "openness" of the system in question.

Classicality is then characterized by the *de facto* inaccessibility, an effective *environment-induced superselection rule* [8], which excludes the vast majority of the states, in principle, contained in the Hilbert space of the system. If this idea is to be viable, one should be able to (at the very least) demonstrate by means of simple models that the process of negative selection described above is (1) efficient and (2) that its outcome is compatible with our first-hand experience of "classical reality." The discussion of such a specific model, a harmonic oscillator interacting with a heat bath of environment harmonic oscillators (investigated before by many authors [12]), is the purpose of this paper.

Early discussions of decoherence [8] focused on idealized models where the self-Hamiltonian of the system H_s was either completely neglected (as is usually the case in models of quantum measurements, where the "to-be-classical" quantum system of interest is the apparatus) or was assumed codiagonal with the interaction Hamiltonian $H_{\rm int}$. The eigenspaces of $H_s+H_{\rm int}$ were then completely unaffected by the evolution. They constituted an obvious "pointer basis," and the corresponding "pointer observable" $\hat{\Lambda}$ satisfied the commutation relation

$$[H_s+H_{\rm int},\hat{\Lambda}]=0\ . \tag{1}$$

The decay of coherent superpositions between various eigenspaces of the pointer basis states was identified with the rate at which reduction of the wave packet was accomplished. It was then argued [8–10] that a sufficiently rapid decay rate enforced an effective environment-induced superselection rule which made only a subset of the Hilbert space, the long-lived pointer states, accessible to observers.

The success of this program in the context of quantum measurement theory, where the transition between quantum and classical domains is perhaps the most dramatic, has encouraged the idea that decoherence is always the key to understanding the emergence of a classical domain from within the presumably quantum "substrate." However, in such a more general setting, the idealized as-

*Electronic address: paz@eagle.lanl.gov
†Electronic address: habib@eagle.lanl.gov
‡Electronic address: whz@eagle.lanl.gov

sumptions appropriate for simplified "gedanken experiments" considered in quantum measurement theory are no longer appropriate. In particular, while one can still appeal to the environment, a set of nontrivial observables which simultaneously commute with both the self- and interaction Hamiltonians is not likely to exist. Thus, all of the states in the Hilbert space will be "degraded" by the evolution to some extent [13]. However, the preferred basis can still be found because the rates at which different states "degrade" will be very different. Therefore, the "pointer states" of the system can be selected by a "predictability sieve" [13]: they are the ones least affected by the interaction with the environment.

We shall demonstrate that, even though in the presence of a self-Hamiltonian that does not commute with the interaction, the nature of the pointer states is not obvious, the role of the observable codiagonal with $H_{\rm int}$ is still important. In the model we will study here, the interaction Hamiltonian will be taken to be proportional to the position x of a particle. However, for this same model the pointer states selected through the "predictability sieve" turn out to be minimum uncertainty coherent states. This result (which will be explicitly demonstrated and discussed in a separate paper [14]) implies that, in weakly damped systems, pointer states are, in some sense, as close to position as to momentum eigenstates. Therefore, it is natural to ask if position, the choice for the pointer observable suggested by $H_{\rm int}$ alone, is really a preferred observable in this model and if so, in what sense. We shall show that this is indeed the case by considering initial states for the system consisting of superpositions of coherent states which differ in position and momentum. We will compute the decoherence rate for such states (which was first computed in [15] in a simplified version of the model which is considered much more carefully in this paper) and show that, as expected, superpositions of spatially separated states decohere much faster than those of states which only differ in their momentum content.

When trying to compute the decoherence time scale, one naturally faces the problem of having to define a reasonable "measure of the effectiveness" of decoherence (i.e., a function that quantifies the importance of interference effects). We will define such a measure using the Wigner function rather than the density matrix. It will be based on the peak-to-peak ratio between the interference and the direct terms (a quantity which is related to the so-called "fringe visibility function" [16]). We will compare this measure with other measures of coherence loss previously used in the literature.

The discussion of decoherence has been usually conducted under the simplest possible set of assumptions, e.g., an Ohmic environment in the often physically unrealistic (but mathematically convenient) high-temperature limit [12]. In this limit it is possible to obtain a simple expression for the rate of decay of the terms of the density matrix which are off-diagonal in the basis of Gaussian coherent states [15]:

$$\tau_D^{-1}=\gamma\left[\frac{\Delta x}{\lambda_{\rm dB}}\right]^2 . \tag{2}$$

In the above, $\lambda_{\rm dB}$ is the thermal de Broglie wavelength, Δx is the separation between the two Gaussian peaks, and γ is the relaxation rate of the system. The most useful tool in studies of decoherence is the quantum master equation describing evolution of the statistical operator of the "oscillator of interest." Such an equation has been derived under less and less constraining assumptions by a number of authors. Notably, Caldeira and Leggett [12] have used the influence functional technique to arrive at the high-temperature Markovian limit. More general equations, valid at arbitrary temperatures, and with time-dependent coefficients, have been obtained in Refs. [17–19]. We will employ the most general results based on the discussion in Ref. [19] to study decoherence for temperatures lower than those mandated by the high-temperature limit. In these cases we will investigate the accuracy of the above approximation for the decoherence rate.

The techniques we use allow us to study the effects produced by very general environments characterized by general frequency distributions (and arbitrary temperatures). One of the important questions still unanswered relates to the conditions an environment should satisfy in order to be able to produce decoherence. In other words, given a closed system, what are the natural splittings into subsystems and environments (or coarse grainings) such that classical behavior arises in one of them? By varying the spectral density of the environment in our model, and studying the dependence of decoherence on these variations, we attempt to gain a deeper understanding of some of the aspects of this issue.

A discussion of the model and the explicit form of the density matrix evolved from an initial superposition of Gaussian states will be the subject of the next section. Numerical results will be presented in Sec. III and a discussion of their relevance for various aspects of the quantum to classical transition will be given in Sec. IV. We end with some concluding remarks in Sec. V.

II. THE PROBLEM AND ITS SOLUTION

A. The model

We will deal with one of the most popular models used to describe the interaction between a quantum system and its environment. The system is taken to be a particle moving in one dimension while the environment is modeled by a collection of harmonic oscillators. The action describing the model is

$$S[x,q_n]=\int_0^t ds\left[\frac{1}{2}M(\dot{x}^2-\Omega_0^2x^2)+\sum_n\frac{1}{2}m_n(\dot{q}_n^2-\omega_n^2q_n^2)-\sum_n C_nxq_n\right], \tag{3}$$

where x is the system coordinate and the q_n are coordinates of the environment oscillators. As is obvious from (3), all nonlinearities are neglected and the particle is therefore just an harmonic oscillator (the cases of a free particle and an unstable oscillator are equally tractable).

This simplification allows us to solve the problem exactly but does not prevent the solution from having interesting nontrivial properties.

It is well known that not all the constants entering in the environment action (3) affect the evolution of the system. In fact, the effect of the environment on the reduced dynamics is contained completely in one function constructed from the constants entering in (3). This function is related to the number density of oscillators with a given frequency present in the environment and to the strength of the coupling between these oscillators and the system. It is called the "spectral density" of the model and is defined as

$$I(\omega)=\sum_n \frac{C_n^2}{2m_n\omega_n}\delta(\omega-\omega_n) . \tag{4}$$

The environment induces noise and dissipation in the reduced dynamics of the system. These two effects are entirely determined by the spectral density (and eventually also by the initial conditions). Therefore, two environments defined by two different actions but possessing the same spectral density are equivalent from the point of view of the system that interacts with them. In this paper we will consider environments that have a spectral density of the form

$$I(\omega)=\frac{2m\gamma_0}{\pi}\frac{\omega^n}{\Lambda^{n-1}}\exp\left[-\frac{\omega^2}{\Lambda^2}\right] , \tag{5}$$

where γ_0 is a constant and Λ is a high-frequency cutoff. The above choice is widely used in the literature to model various physical situations. The environments described by (5) are known as sub-Ohmic ($n<1$), Ohmic ($n=1$), or supra-Ohmic ($n>1$) depending on the form of the spectral density in the low-frequency ($\omega\ll\Lambda$) part of the spectrum. In particular, we will consider the $n=1$ and 3 examples. The first of these choices is the one most studied in the literature and produces a dissipative force that, in the limit of $\Lambda\to\infty$, is proportional to the velocity. The case $n=3$ is a prototypical example of a supra-Ohmic environment that is used to model the interaction between defects and phonons in metals (see Refs. [20,21]) and also to mimic the interaction between a charge and its own electromagnetic field [22].

B. Initial conditions

We will assume that the system and the environment are initially uncorrelated. The total density matrix then factorizes into a product of a function of the system variables and another function of the environment variables. We will further assume that the initial state of the environment is one of thermal equilibrium at a given temperature T.

As we are interested in analyzing decoherence (following the discussion in Sec. I), we will consider an initial state for the system that consists of the following superposition of coherent states (we set $\hbar=1$ throughout the paper):

$$\Psi(x,t=0)=\Psi_1(x)+\Psi_2(x) , \tag{6}$$

where

$$\Psi_{1,2}(x)=N\exp\left[-\frac{(x\mp L_0)^2}{2\delta^2}\right]\exp(\pm iP_0x) , \tag{7}$$

$$N^2\equiv\frac{\bar{N}^2}{\pi\delta^2}=\frac{1}{2\pi^2\delta^2}\left[1+\exp\left[-\frac{L_0^2}{\delta^2}-\delta^2P_0^2\right]\right]^{-1} . \tag{8}$$

Note that we assumed (just for simplicity) that the two initial wave packets are symmetrically located in phase space and that the relative phase is zero. These assumptions are visually manifest in Fig. 1 where we have plotted the initial Wigner function [23], defined in terms of the density matrix as

$$W(x,p)=\int_{-\infty}^{+\infty}\frac{dz}{2\pi}e^{ipz}\rho(x-z/2,x+z/2) , \tag{9}$$

for two special initial conditions: Fig. 1(a) corresponds to the case $L_0=5\delta$, $P_0=0$ which, in what follows, will be called condition A while Fig. 1(a') corresponds to $L_0=0$, $P_0=5/\delta$ (condition A'). We consider conditions A and A' as two extreme cases that will allow us to study the dependence of decoherence on the initial condition of the system (the coherent states are spatially separated for A while for A' they are separated in momentum). The above two initial conditions share the common feature that, as a consequence of quantum interference, the Wigner function oscillates and becomes negative in some regions of phase space (and therefore cannot be interpreted as a probability distribution).

More generally we could consider nonsymmetric initial conditions for which the wave packets Ψ_i are centered about the position L_i and the momentum P_i. In this case the graph of the initial Wigner function turns out to be identical to the one shown in Fig. 1 provided we shift the origin to the point centered between the two wave packets [whose coordinates are $x_m=(L_1+L_2)/2$ and $p_m=(P_1+P_2)/2$] and use the relative coordinate and momentum as the values of L_0 and P_0 (i.e., $L_0=L_1-L_2$, $P_0=P_1-P_2$).

C. Time evolution

The above model is linear and the initial condition is Gaussian. Consequently it can be solved exactly for an environment with a general spectral density in an initial state with arbitrary temperature. Here we briefly describe only the general features of the solution as it has been extensively treated in the literature (see, e.g., Ref. [20]). One of the possible ways in which the exact solution can be obtained is by using the form of the evolution operator for the reduced density matrix (the reduced density matrix is the full density matrix traced over the environment variables: it depends only on the system variables). This propagator, which we denote by $J(t;t_0)$, operates in the following manner:

$$\rho_{\rm red}(x,y,t)=\int\int dx_0dy_0J(x,y,t;x_0,y_0,t_0)\times\rho_{\rm red}(x_0,y_0,t_0) , \tag{10}$$

and can be written in a path-integral representation as

$$J(x,y,t|x_0,y_0,t_0)$$
$$=\int_{x_0}^{x}D\bar{x}\int_{y_0}^{y}D\bar{y}\exp\left[\frac{i}{\hbar}\{S[\bar{x}]-S[\bar{y}]\}\right]F[\bar{x},\bar{y}]\ , \quad (11)$$

where $F[x,y]$ is the Feynman-Vernon influence functional that arises due to the integration over the environment variables. For the model we are considering, this functional is well known and can be written as (see Ref. [20])

$$\ln(F[x,y])=\int_0^t ds\int_0^s ds'(x-y)(s)$$
$$\times[-i\eta(s-s')(x+y)(s')$$
$$-\nu(s-s')(x-y)(s')]\ , \quad (12)$$

where $\nu(s)$ and $\eta(s)$ are the noise and dissipation kernels defined in terms of the spectral density:

$$\eta(s)=-\int_0^\infty d\omega\, I(\omega)\sin(\omega s)\ ,$$
$$\nu(s)=\int_0^\infty d\omega\, I(\omega)\coth\left[\frac{\omega}{2k_BT}\right]\cos(\omega s)\ . \quad (13)$$

As the integrand of (11) is Gaussian, the integral can be computed exactly. Written in terms of the variables $\xi=x-y$ and $X=x+y$, the result is

$$J(X,\xi,t;X_0,\xi_0,t_0)=\frac{b_3}{2\pi}\exp(-a_{11}\xi^2-a_{12}\xi\xi_0-a_{22}\xi_0^2)$$
$$\times\exp(ib_1X\xi+ib_2X_0\xi-ib_3X\xi_0$$
$$-ib_4X_0\xi_0)\ , \quad (14)$$

where the functions $b_k(t)$ and $a_{ij}(t)$ depend on the environment and can be constructed in terms of solutions to the equation

$$\ddot{u}(s)+\Omega_0^2u(s)+2\int_0^s ds'\eta(s-s')u(s')=0\ . \quad (15)$$

If u_1 and u_2 are two solutions of (15) that satisfy the boundary conditions $u_1(0)=u_2(t)=1$ and $u_1(t)=u_2(0)=0$, then the functions that appear in (14) are

$$2b_1(t)=\dot{u}_2(t)\ ,$$
$$2b_3(t)=\dot{u}_2(0)\ ,$$
$$2b_2(t)=\dot{u}_1(t)\ , \quad (16)$$
$$2b_4(t)=\dot{u}_1(0)\ ,$$

$$a_{ij}(t)=\frac{1}{1+\delta_{ij}}\int_0^t\int_0^t dsds'u_i(s)u_j(s')\nu(s-s')\ , \quad (17)$$

where the overdot signifies differentiation with respect to s. Note that the functions $b_i(t,t_0)$ $\{i=1,\ldots,4\}$ depend only on the spectral density while the $a_{ij}(t,t_0)$ $\{i,j=1,2\}$ are functions both of the spectral density and the temperature.

Knowing the form of the propagator (14) and the initial condition for the reduced density matrix [obtained from (6)] we can compute the reduced density matrix at an arbitrary time (it is simply a matter of calculating several Gaussian integrals). After a straightforward but somewhat tedious calculation we can show that the Wigner function can always be decomposed into two Gaussian peaks and an interference term:

$$W(x,p,t)=W_1(x,p,t)+W_2(x,p,t)+W_{\rm int}(x,p,t)\ , \quad (18)$$

where

$$W_{1,2}(x,p,t)=\frac{\bar{N}^2}{\pi}\frac{\delta_2}{\delta_1}\exp\left[-\frac{(x\mp x_c)^2}{\delta_1^2}\right]$$
$$\times\exp[-\delta_2^2(p\mp p_c-\beta(x\mp x_c))^2]\ , \quad (19)$$

$$W_{\rm int}(x,p,t)=2\frac{\bar{N}^2}{\pi}\frac{\delta_2}{\delta_1}\exp(-A_{\rm int})$$
$$\times\exp\left[-\frac{x^2}{\delta_1^2}-\delta_2^2(p-\beta x)^2\right]$$
$$\times\cos[2\kappa_p p+2(\kappa_x-\beta\kappa_p)x]\ , \quad (20)$$

and

$$\delta_1^2=\left[a_{22}+\frac{1}{4\delta^2}+\delta^2b_4^2\right]b_3^{-2}\ , \quad (21)$$

$$\delta_2^{-2}=4\left[a_{11}+\delta^2b_2^2-\frac{1}{4\delta_1^2}\left[\frac{a_{12}-2\delta^2b_2b_4}{b_3}\right]^2\right]\ , \quad (22)$$

$$\beta=2b_1+\frac{a_{12}-2\delta^2b_2b_4}{\delta_1^2b_3}\ , \quad (23)$$

$$\kappa_x=-\frac{1}{2\delta_1^2b_3}\left[\frac{L_0}{\delta^2}+2\delta^2P_0b_4\right]\ , \quad (24)$$

$$\kappa_p=\delta_2^2\left[2\delta^2P_0b_2+\left[\frac{L_0}{\delta^2}+2\delta^2b_4P_0\right]\right.$$
$$\left.\times\left[\frac{a_{12}-2\delta^2b_2b_4}{2\delta_1^2b_3^2}\right]\right]\ , \quad (25)$$

$$x_c=\frac{P_0-2L_0b_4}{2b_3}\ , \quad (26)$$

$$p_c=2x_cb_1+2L_0b_2\ , \quad (27)$$

$$A_{\rm int}=\frac{L_0^2}{\delta^2}+\delta^2P_0^2-\frac{\kappa_p^2}{\delta_2^2}-\delta_1^2\kappa_x^2\ . \quad (28)$$

Expressions (19) and (20) are the main results exploited in this paper. The form of the Wigner function at the initial time is recovered from the above equations by using the initial conditions

$$\delta_1^2=\delta_2^2=\delta^2\ ,$$
$$\kappa_x=P_0=p_c,\quad \kappa_p=L_0=x_c\ , \quad (29)$$
$$A_{\rm int}=0\ .$$

If we consider a nonsymmetric initial condition the

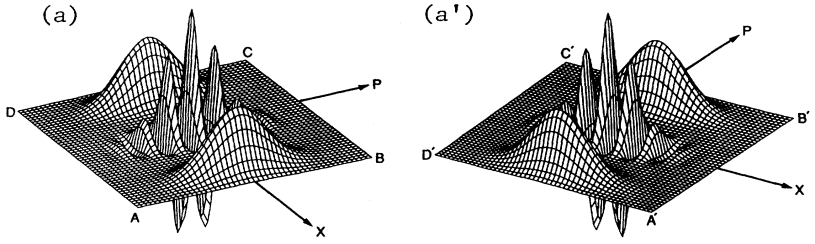

FIG. 1. The Wigner function corresponding to the initial conditions A (a): $L_0=5\delta_0$, $P_0=0$, and A' (a'): $L_0=0$, $P_0=5/\delta_0$. The coordinates of the points B and B' are $(x=7,p=4)$ and $(x=4,p=7)$ respectively. The interference between the two wave functions is responsible for the oscillations.

above expressions are modified in a very simple way. In fact, the Wigner function for the nonsymmetric case $W_{\rm ns}(x,p,t)$ can be obtained from the one corresponding to the symmetric case $W_{\rm sym}(x,p,t)$ [which is given by (18)] as

$$W_{\rm ns}(x,p,t)=W_{\rm sym}(x-x_m(t),p-p_m(t),t)\ , \tag{30}$$

where the functions $x_m(t)$ and $p_m(t)$ describe the evolution of the midpoint between the two Gaussian peaks and are defined by

$$x_m=\frac{P_1+P_2-2(L_1+L_2)b_4}{4b_3}\ , \tag{31}$$

$$p_c=2x_m b_1+2(L_1+L_2)b_2\ . \tag{32}$$

D. Analysis of the solution and the decoherence process

Having already presented the basic technical ingredients of our method, in this subsection we will pay attention to two, more conceptual, aspects. We will first study the general features of the evolution of the Wigner function and will later define and describe the "measure of the effectiveness" of decoherence appropriate to this problem. We will analyze its properties and compare then with those of other possible choices.

From the solution given above, it is possible to immediately gain some qualitative understanding of the behavior of the Wigner function. Let us consider first a symmetric initial condition (i.e., $x_m=0=p_m$) and analyze the two direct terms in (18). The center of each of the two Gaussian packets $W_{1,2}(x,p)$ follows a trajectory given by the equations $x_{1,2}=\pm x_c$ and $p_{1,2}=\pm P_c$ which, as can be seen from (26) and (27), depend only on the spectral density of the environment and not on the temperature. The temperature affects the shape of these packets through its influence on the variances δ_1 and δ_2 as well as on the function β. The shape of the "isodensity" ($W_i=$const) contours of an individual Gaussian wave packet is always an ellipse that may rotate in time due to the presence of β. Apart from this rotation ("shearing"), the state may get squeezed due to the changes in the values of $\delta_{1,2}$ induced by the interaction with the environment. The area of the rotating ellipse is always equal to $\pi\delta_1/\delta_2$ which may also vary with time (note that the peak value of $W_{1,2}$ is inversely proportional to $\pi\delta_1/\delta_2$). We will later study examples of environments for which some (or all) of these effects are clearly seen. The effect of the environment on $W_{\rm int}(x,p)$ can also be examined using (20). From that equation, we see that the peak value of $W_{\rm int}(x,p)$ (in our case the peak is always at the origin due to the symmetry of the initial conditions but this does not have to be the case), the wavelength of the oscillations, and their orientation are all affected in a temperature-dependent manner.

Starting from the initial conditions A and A' [see Figs. 1(a) and 1(a')], we have numerically computed for various environments the time evolution of the functions that enter in (19) and (20). We will present the results in the next section but would like to discuss our method of analysis here. In order to do so, it will be useful to have in mind the concrete example shown in Figs. 2(a)–2(d) and 2(a')–2(d'). These figures correspond to the evolution of the Wigner function of a harmonic oscillator

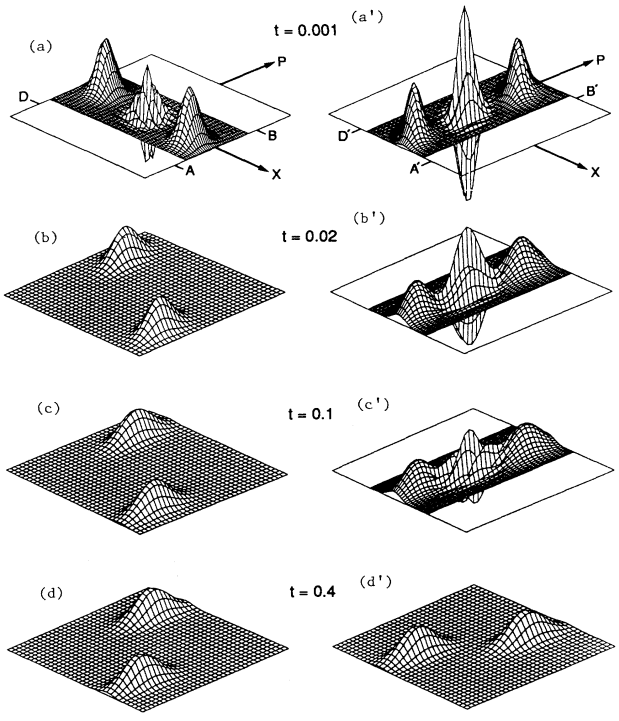

FIG. 2. The time evolution of initial conditions A and A'. The oscillations disappear faster in the first case since the environment can distinguish between the two peaks. In the second case, the interference is damped over a dynamical time scale.

whose renormalized frequency is set to unity (i.e., all times are measured in units of $\Omega_{\rm ren}^{-1}$). This oscillator is in contact with an Ohmic environment characterized by a spectral density of the form (5) with $n=1$. The dissipation constant is taken to be $\gamma_0=0.3$ so the oscillator is underdamped, and the high-frequency cutoff set to $\Lambda=500$. The initial state of the environment is the vacuum (zero temperature). As we see from these figures, for late times (i.e., times of the order of the dynamical scale) the effect of the interference is washed out by the interaction with the environment. This occurs for both the initial conditions we considered. However, it is also evident [see Figs. 2(b) and 2(b′)] that decoherence is much faster in the first case. The effect of the interaction with the environment is much more pronounced for condition A where the centers of the two Gaussian wave packets are initially separated in position. In this case, the interference is damped very rapidly. Moreover, the system feels an initial kick that has no direct effect on decoherence but affects the dynamics of the system. Initially, it noticeably moves the centers of the Gaussian packets closer to the origin.

To quantitatively analyze decoherence in a situation such as the one described above we need to define a function that allows us to quantify the importance of the interference at a given time. As our diagnostic tool we will use the peak-to-peak ratio between the interference and the direct terms in the Wigner function, a quantity which is determined by $A_{\rm int}$, and is related to the so-called "fringe visibility function:"

$$\exp(-A_{\rm int})=\frac{1}{2}\frac{W_{\rm int}(x,p)|_{\rm peak}}{[W_1(x,p)|_{\rm peak}W_2(x,p)|_{\rm peak}]^{1/2}} . \tag{33}$$

A close analysis of the definition of $A_{\rm int}$ given in (28) shows that this function vanishes initially and is always bounded from above, i.e.,

$$A_{\rm int}\le\frac{L_0^2}{\delta^2}+\delta^2P_0^2=A_{\rm int}|_{\rm max} . \tag{34}$$

The value of $A_{\rm int}$ cannot grow to infinity as a consequence of the fact that the two Gaussian initial states have a finite overlap which is proportional to $\exp(-A_{\rm int}|_{\rm max})$. The process of decoherence destroys the potential for interference between the states of the preferred "pointer basis," which is measured by the size of the off-diagonal terms of the density matrix in that basis. As $A_{\rm int}$ grows, the interference effects become less and less important, and the state of the system becomes closer to a mixture of the pointer states. Because of the simplicity of the initial conditions we are considering, $A_{\rm int}$ seems to be a good measure of the efficiency of decoherence and we can say that such a process is indeed completed when $A_{\rm int}$ becomes much larger than unity and then remains $\gg 1$ over dynamical time scales.

We will soon discuss some of the advantages of $A_{\rm int}$ as a measure of the effectiveness of decoherence. Now we turn to some other candidates that can be proposed to play this role. One of them is simply the entropy $S=-{\rm Tr}(\rho_{\rm red}\ln\rho_{\rm red})$, the calculation of which is rather complicated for the initial conditions we study here. In our case it is much simpler to compute the linear entropy $S_{\rm lin}=1-{\rm Tr}(\rho_{\rm red}^2)$ which is an important quantity in its own right: $S_{\rm lin}$ provides us with information about the degree of mixing generated by the interaction with the environment. For an initial pure state such as (6) the linear entropy vanishes while for a mixture of two orthogonal states (with equal probability) it is equal to $\frac{1}{2}$. Thus, if the interaction with the environment is such that interference is suppressed, we should observe the linear entropy growing from its initial vanishing value to a value which should be close to one-half. This is indeed what happens in many of the cases we analyzed where the conclusions reached by using $A_{\rm int}$ as an indicator of decoherence were almost the same as the ones obtained using the linear entropy as a diagnostic tool. However, in some other cases $S_{\rm lin}$ was not as sensitive a measure of the decay of the off-diagonal terms as $A_{\rm int}$. The reason for this is simple to understand: $A_{\rm int}$ is a "relative" quantity that compares the effect of the environment on the interference terms to the one it produces on the direct terms. On the other hand, the linear entropy is an "absolute" quantity that may vary simply because the direct terms $S_{\rm lin1,2}=1-{\rm Tr}\rho_{1,2}^2$ depend on time [note that for Gaussian wave packets ${\rm Tr}\rho_{1,2}^2$ is inversely proportional to the area inside the curves defined by the equation $W_{1,2}=$const and that this area grows with time due to the interaction with the environment: if the system approaches a thermal equilibrium the final value of the area is proportional to $(k_BT/\hbar\Omega)2\pi\hbar$]. One can also define a quantity related to the entropy contrast,

$$C={\rm Tr}(\rho^2)/[{\rm Tr}(\rho_1^2){\rm Tr}(\rho_2^2)]^{1/2} ,$$

and show that its behavior is always qualitatively similar to that of $A_{\rm int}$.

As remarked above (and as illustrated in Fig. 2) the rate of the decoherence process strongly depends on the initial condition. Any reasonable measure of the effectiveness of decoherence must be able to distinguish between the evolutions illustrated in Fig. 2. As is evident from (28), $A_{\rm int}$ does depend on the initial condition and turns out to have a drastically different behavior for conditions A and A' (much the same happens with $S_{\rm lin}$). We remark here that some other naively reasonable measures have to be ruled out as they turn out to be rather insensitive to initial conditions. For example, one may notice that the structure of the reduced density matrix is such that the diagonal elements of the interference term satisfy

$$\rho_{\rm int}(x,x,t)=2[\rho_1(x,x,t)\rho_2(x,x,t)]^{1/2}\times\exp[-B_{\rm int}(t)]\cos\chi(x,t) , \tag{35}$$

and as a diagnostic tool for decoherence attempt to use the function $B_{\rm int}$ (in fact, this was done in Ref. [24]). However, it is easy to show that this function depends on the initial conditions in a rather trivial way:

$$B_{\rm int}(t)=\left[\frac{L_0^2}{\delta^2}+\delta^2P_0^2\right]\left[\frac{a_{22}}{a_{22}+(1/2)\delta^{-2}+\delta^2b_4^2}\right] . \tag{36}$$

Therefore, the behavior of $B_{\rm int}(t)$ is identical for conditions A and A' and we have to conclude that it is a very bad candidate to measure the potential for interference (especially for the case $L_0=0$). Something similar would occur if, instead of using the peak-to-peak ratio between the interference and the direct terms in the Wigner function, we try to use simply the ratio between them. Indeed it is possible to prove that $W_{\rm int}(x,p,t)$ can be always written as

$$W_{\rm int}(x,p,t)=2[W_1(x,p,t)W_2(x,p,t)]^{1/2} \times\exp\left[-\left[\frac{L_0^2}{\delta^2}+\delta^2 P_0^2\right]\tilde{B}_{\rm int}(t)\right] \times\cos[\alpha(x,p,t)] ,$$

where $\tilde{B}_{\rm int}(t)$ is a function that does not depend on the initial conditions. Therefore, $\tilde{B}_{\rm int}(t)$ cannot properly describe the decoherence process.

In the case of nonsymmetric initial conditions, very little of the above discussion has to be changed. In particular, as is clear from definition (33), the function $A_{\rm int}$ is the same in both cases and depends only upon the initial values of the relative coordinate L_0 and momentum P_0. This is an obvious consequence of the fact that, due to the linearity of the model, the interaction with the environment does not introduce a preferred position in the system (but still makes position a preferred observable) since the influence functional (12) is invariant under translations. Thus, decoherence in the nonsymmetric case takes place exactly in the same way as in the symmetric case.

What are the physical processes that affect the value of $A_{\rm int}$? To get a flavor of the time evolution of this function it is very helpful to remember that for a harmonic oscillator the Wigner function obeys an equation of the Fokker-Planck type. This important result is valid for a linearly coupled environment characterized by a generic spectral density in an initial state of arbitrary temperature. In fact, as was recently proven in Ref. [19], this equation can always be written as

$$\dot{W}=-\{H_{\rm ren}(t),W\}_{\rm PB}+2\gamma(t)\partial_p(pW) +D(t)\partial_{pp}^2 W-f(t)\partial_{px}^2 W , \tag{37}$$

where the first term on the right-hand side is a Poisson bracket. All the coefficients that appear in this equation [i.e., the friction $\gamma(t)$, the diffusion coefficients $D(t)$ and $f(t)$, as well as the frequency renormalization that is contained in the renormalized Hamiltonian $H_{\rm ren}(t)$] are time-dependent functions that strongly depend on the spectral density of the environment (the diffusion coefficients also depend on the temperature). From definition (33) we can compute the time derivative of $A_{\rm int}$:

$$\dot{A}_{\rm int}=\frac{\dot{W}_{\rm int}}{W_{\rm int}}\bigg|_{\rm peak}-\frac{1}{2}\left[\frac{\dot{W}_1}{W_1}+\frac{\dot{W}_2}{W_2}\right]\bigg|_{\rm peak} , \tag{38}$$

which, using the Fokker-Planck equation, can be transformed into

$$\dot{A}_{\rm int}=D(t)\kappa_p^2-2f(t)\kappa_p(\kappa_x-\beta\kappa_p) . \tag{39}$$

This simple (and exact) equation shows that the evolution of $A_{\rm int}$ depends very strongly on diffusion effects [that explicitly appear in the right-hand side of (39)] but rather weakly on friction or free evolution. These two effects only change $A_{\rm int}$ indirectly through their impact on κ_x and κ_p [note that the two first terms on the right-hand side of the Fokker-Planck equation (37) do not contribute to (39)]. In fact, while there are two time scales affecting the evolution of $W_{\rm int}$ [a dynamical time set by the combined effect of $H_{\rm ren}$ and γ, as well as the diffusion time determined by $D(t)$] only one affects $A_{\rm int}$ since the dynamical contribution is canceled out by the last two terms in (38). The normal diffusion always results in decoherence since the first term in the right-hand side of (39) is positive. This term is proportional to κ_p^2 which, as can be seen from (20), is related to the wavelength λ of the oscillations in the Wigner function:

$$\kappa_p=\frac{2\pi}{\lambda}\cos\theta , \tag{40}$$

where θ is the angle between the p axis and the axis along which the Wigner function oscillates. On the other hand, the contribution of the anomalous diffusion [the last term in (37)] to decoherence does not have a definite sign since the signature of the second term in (39) depends on the relation between κ_p and κ_x. The dependence of $A_{\rm int}$ upon the initial condition enters (39) through κ_p and κ_x whose initial values are determined by (29).

To better understand the main features of the evolution of $A_{\rm int}$ in some very important cases we will solve the evolution equation (39) approximately assuming that the normal diffusion dominates the right-hand side. This happens in the widely studied case of an Ohmic environment in the high-temperature regime (where $D\propto T$ and $f\propto T^{-1}$). However, we must stress that, in other cases, the anomalous diffusion can be important and its effects can be observed (if not experimentally, at least theoretically). This can happen, for instance, when κ_p is small. [Note also that the right-hand side of (39) is zero when κ_p vanishes.] For some environments (such as $n=1$ at low temperature), close to the time when $\kappa_p=0$, the effect of the anomalous diffusion can be such that the value of $A_{\rm int}$ may locally decrease. This effect will be illustrated in the next section.

Starting from condition A, where the ripples in the Wigner function are initially oriented along the p axis, we will assume that the decoherence process occurs on a time scale much shorter than the dynamical scale, and that during this time the interference fringes remain oriented along the p axis. Using the Fokker-Planck equation, it is now a simple matter to derive an equation for the wavelength λ of the interference oscillations:

$$\frac{d}{dt}\lambda=-4D\delta_2^2\lambda . \tag{41}$$

Equation (37) also allows us to show that, under the above assumptions, the evolution of δ_2 (which is simply related to the momentum dispersion of a single Gaussian

packet) is given by $\delta_2^{-2}=\delta^2+4Dt$. Then (41) can be easily integrated and the result used to obtain

$$A_{\rm int}(t)\simeq L_0^2\frac{4Dt}{1+4D\delta^2 t} . \tag{42}$$

This equation can essentially be thought of as being a high-temperature (and low damping) approximation of the behavior of $A_{\rm int}$. One of the most remarkable features of (42) is that it describes the approach to the correct asymptotic value $A_{\rm int}|_{\rm max}$ in a time scale that is entirely unrelated to the relaxation time scale of the system. This confirms the suspicion that, as we argued before, $A_{\rm int}$ evolves on a time scale which is more or less independent of any dynamical scale. In contrast, the approach to equilibrium of other quantities (such as the variances δ_1 and δ_2) can also be described by the Fokker-Planck equation (37) but the characteristic time scale governing this process is fixed by the friction coefficient γ (i.e., these quantities do not approach their asymptotic value if one neglects friction).

In the next section we will compare the high-temperature approximation (42) with the results obtained from the numerical calculation of $A_{\rm int}$ and find the circumstances under which (42) is a reasonable approximation. From (42) it is easy to derive a decoherence rate $\Gamma_{\rm dec}=1/t_{\rm dec}$, where $t_{\rm dec}$ is such that $A_{\rm int}(t_{\rm dec})=1$. This rate is given by

$$\Gamma_{\rm dec}=4L_0^2D\left[1-\frac{\delta^2}{L_0^2}\right] . \tag{43}$$

For the Ohmic environment at high temperatures, the diffusion coefficient $D=2\gamma_0 mk_BT$. Replacing this value in (43) we obtain

$$\Gamma_{\rm dec}=8L_0^2\gamma_0 k_BT \tag{44}$$

in agreement with the estimate [15] previously obtained by one of us.

III. NUMERICAL RESULTS

A. The method

We will examine here the numerical results obtained for two different classes of environment. First we will treat the Ohmic case which is characterized by a spectral density given by (5) with $n=1$. Later we will consider a typical supra-Ohmic case corresponding to $n=3$ in (5). We will present data extracted from numerical calculations and compare them with some analytic estimates. In particular, we will analyze the behavior of $A_{\rm int}$ and of the decoherence rate and confront the approximations discussed in the previous section with the numerical results.

The major part of the computation consists of calculating the time-dependent coefficients that appear in the propagator, i.e., $b_k(t)$ and $a_{ij}(t)$. Our numerical scheme is based on solving the integrodifferential equation (15) for $u_{1,2}$. We do this by using a shooting method that allows us to impose the appropriate boundary conditions.

In some cases, it is actually possible to find a local approximation to Eq. (15). In fact, for the $n=1,3$ environments, by neglecting the existence of the high-frequency cutoff in the spectral density (5), the dissipation kernel is transformed into a distribution that can be related to the Dirac δ function (or some derivative of it). In this way (15) can be transformed into a differential equation that may be analytically solved by ordinary methods. The functions $u_{1,2}^{\rm app}$ found in this way are good approximations to the true solutions of the nonlocal equations for times much longer than the one fixed by the cutoff frequency. However, for earlier times the true solutions must be obtained from the nonlocal equation. Comparing the exact and approximate solutions we have found that, for times larger than $\sim 100\Lambda^{-1}$, the two coincide to a very high accuracy (10^{-5}). We point out that the trick of using a local approximation for (15) may work only for some special environments (such as those considered in this paper) but may be totally useless for situations where the dissipative kernel is intrinsically nonlocal (as, for instance, in the sub-Ohmic case or in environments with noninteger exponents).

B. Ohmic environment

This environment [which corresponds to $n=1$ in (5)] is undoubtedly the most popular one found in the literature. The local approximation of (15) is very simple in this case: disregarding the high-frequency cutoff in (5), the dissipation kernel (13) becomes proportional to the first derivative of the Dirac δ function. The local approximation to (15) then becomes

$$\ddot{u}(s)+2\gamma_0\dot{u}(s)+\Omega_{\rm ren}^2u(s)=-4\gamma_0\delta(s)u(0) , \tag{45}$$

where the renormalized frequency is $\Omega_{\rm ren}^2=\Omega_0^2+\Delta\Omega^2$ with $\Delta\Omega^2=-4\gamma_0\delta(0)=-4\gamma_0\Lambda\pi^{1/2}$. The effects introduced by the environment in the above equation are threefold: it not only dresses the bare oscillator renormalizing its frequency but also introduces friction [produced by the second term in the left-hand side of (45)] and an initial kick [associated by the right-hand side of (45)]. Solving this equation, the behavior of the coefficients in the long-time regime is easily shown to be

$$\begin{aligned} 2b_1(t)&=-2b_4(t)=\tilde{\Omega}\cot(\tilde{\Omega}t)-\gamma_0 ,\\ 2b_3(t)&=-2b_2(t)\exp(2\gamma_0 t)\\ &=\frac{\tilde{\Omega}}{\sin(\tilde{\Omega}t)}\exp(\gamma_0 t) , \end{aligned} \tag{46}$$

where $\tilde{\Omega}=(\Omega_{\rm ren}^2-\gamma_0^2)^{1/2}$. As a side remark we mention that our equations differ slightly from the ones obtained by Caldeira and Leggett in Ref. [12]: since we are solving (15) numerically there is no need to neglect the kick term appearing on the right-hand side of (45) as they did. This term may significantly alter the value of b_4 and affects the motion of the centers of the two wave packets only if $L_0\neq 0$ [it is responsible for the sudden jump of the position of the center of the wave packets observed in Fig. 2(b)] but it has no direct effect on decoherence [in fact, by setting the right-hand side of Eq. (45) to zero, the evolution of $A_{\rm int}$ is almost unchanged]. The functions $a_{ij}(t)$ do not have a simple form even in the local approximation but it is possible to write them as integrals of simple functions.

The use of the local approximation in the very short time scale can lead to rather pathological results. For instance, it is possible to show that the friction coefficient appearing in the Fokker-Planck equation (37) can be written in general as [19]

$$\gamma(t)=-\left[\frac{\dot{b}_2}{2b_2}+b_1\right]. \tag{47}$$

Therefore, using the local approximation (46), we easily conclude that the friction coefficient is equal to the constant γ_0. It can also be shown that in the local approximation the diffusion coefficients D and f, instead of being finite, actually vanish at $t=0$. Therefore, the Fokker-Planck equation with coefficients calculated in the local approximation is friction dominated and can lead to absurd results (as pointed out in Ref. [25]) when applied to judiciously chosen initial conditions beyond the range of its validity. For example, the time evolution can violate the positivity of the reduced density matrix.

We now turn to the time evolution of $A_{\rm int}$. We will always consider an underdamped harmonic oscillator and use units in which $\Omega_{\rm ren}=1$. The high-frequency cutoff is $\Lambda=500$. We first analyze the case $\gamma_0=0.3$ and plot the function $A_{\rm int}$ in Figs. 3(a) and 3(a') for the initial conditions A and A', respectively. We consider three different temperatures, $T_1=0$, $T_2=10$, and $T_3=25\,000$ and also plot the motion of the center of the Gaussian packet $[x(t)=x_c(t)]$.

From Fig. 3 we can extract the first obvious conclusion that has been already advanced: decoherence is considerably faster for condition A than for A'. In fact, it is apparent from our results that for condition A the growth of $A_{\rm int}$ is faster than any dynamical time scale even at very low temperatures. For example, at zero temperature the decoherence time scale is extremely short: $t_{\rm dec}\simeq 10^{-3}$. On the other hand, for the second initial condition decoherence occurs on a dynamical time scale: in the high-temperature regime, $A_{\rm int}$ grows to unity when the centers of the two wave packets become separated by an amount which is approximately $2x_c=0.5$ while in the zero-temperature case this value increases to $2x_c=2$. This is a rather intuitive result since the interaction Hamiltonian is proportional to the coordinate x. The centers of the two wave packets have to separate in position before the environment can effectively distinguish between them. It is in this sense that position is a preferred observable (as previously argued in Refs. [7,9,13]) with condition A being much more sensitive to the environment than condition A'.

A second observation we can make from Fig. 3(a) is that, for low temperatures, the growth of $A_{\rm int}$ becomes considerably slower for intermediate times (of the order of $t=0.6$). In fact, in the zero-temperature case, $A_{\rm int}$ has a local minimum around that time. This can be explained as the effect of the anomalous diffusion term in the Fokker-Planck equation which generates the second term in (28). This effect occurs close to the times where the function κ_p vanishes (i.e., when the oscillations of the Wigner function are oriented along the x axis). At high temperatures, this effect is not observable since the value of the anomalous diffusion is very small (as it is inversely proportional to the temperature [19]). For the initial condition A' the same effect, as seen in Fig. 3(a'), occurs at later times simply because, in this case, κ_p vanishes only after the two centers have made approximately a 180° turn.

We can now ask how good an approximation (42) really is. Obviously, it only makes sense to compare this equation with the results obtained for condition A since the approximations used to derive (42) do not hold for condition A'. In Fig. 4, we plot the function $A_{\rm int}$ [curve (*i*)] and the approximation given by (42) [curve (*ii*)]. The

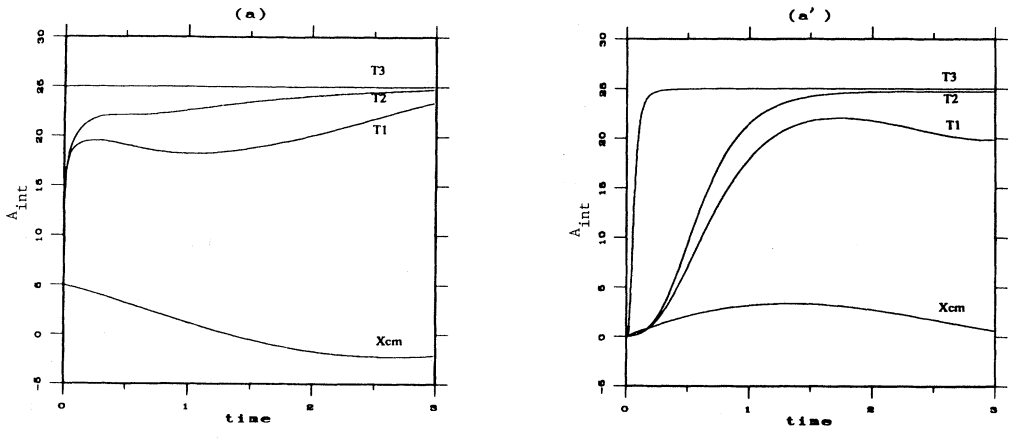

FIG. 3. The evolution of $A_{\rm int}$, which is a measure of the effectiveness of decoherence, for an underdamped harmonic oscillator ($\Omega_r=1$, $\gamma_0=0.3$) in an Ohmic environment at temperatures $T_1=0$, $T_2=10$, and $T_3=25\,000$ (the high-frequency cutoff is $\Lambda=500$). For the initial condition A (a), $A_{\rm int}$ becomes much larger than one in a very short time scale. In the case of A' (a'), the growth of $A_{\rm int}$ takes place in a dynamical time scale (this is clearer in the low-temperature case). In both figures we also display the position of the center of one of the Gaussian packets (note that for condition A the packets are "kicked" by the environment and start moving towards each other).

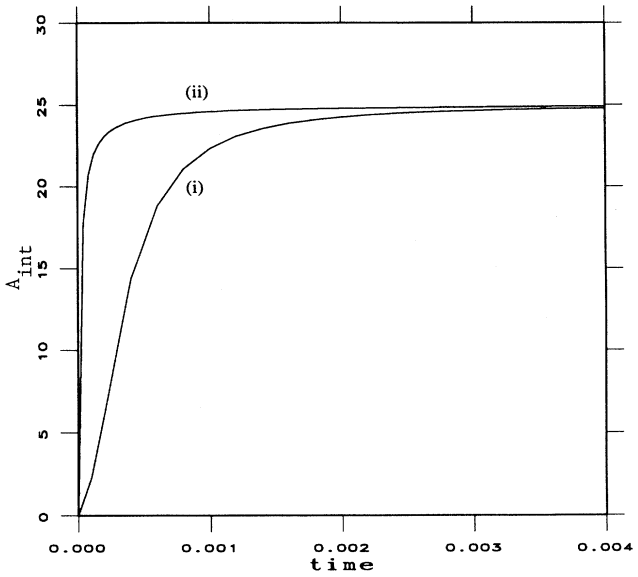

FIG. 4. The short-time evolution of A_{int} in the high-temperature regime. The parameters are the same as in Fig. 3 and we display only the result corresponding to initial condition A. Curve (i) corresponds to our numerical results while curve (ii) was obtained using the high-temperature approximation given by Eq. (38). For curve (i) the asymptotic value of A_{int} is approached in a time scale that is of the order of the collision time $t_\Lambda = 0.002$. The high-temperature approximation fails because it predicts a much shorter decoherence time while the environment cannot react on a time scale shorter than t_Λ.

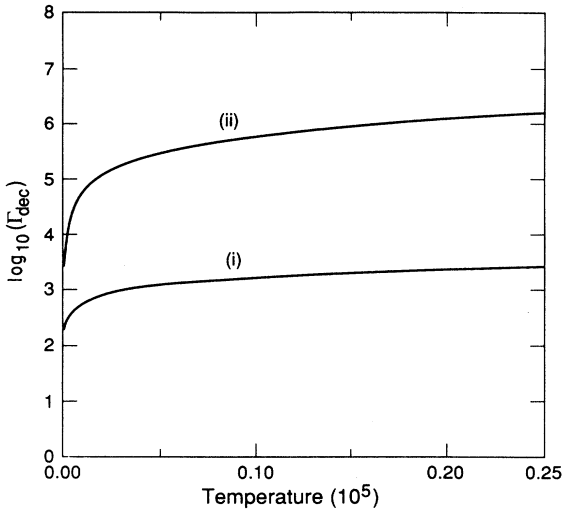

FIG. 5. The decoherence rate calculated numerically [curve (i)] is lower than the one computed using the high-temperature approximation [curve (ii)]. In the high-temperature regime the difference can be 3 orders of magnitude. The reason for the disagreement is that the decoherence rate predicted by the high-temperature approximation [Eq. (39)] turns out to be larger than the one determined by the high-frequency cutoff (which fixes a real physical limit on the time the environment needs to be able to react).

temperature is taken to be $T_3 = 25\,000$ and the time scale of the plot is set much shorter than in the previous examples since we want to examine in detail the region in which the function grows. As we can see, there is some discrepancy between the approximation (42) and the exact result. The approximation predicts decoherence in a shorter time than the one obtained from the numerical results. The discrepancy between the numerical results and the "high-temperature" approximation is more clearly seen by examining Fig. 5 where we have plotted the decoherence rate Γ_{dec} as a function of the temperature. Curve (i) corresponds to our numerical results (we computed the decoherence time t_{dec} for 15 temperatures ranging from zero to T_3) while curve (ii) corresponds to the approximation (43). Note that for temperatures of the order of T_3, the approximation for the rate of decoherence is 3 orders of magnitude larger than our numerical result. At first sight this discrepancy appears paradoxical since the temperatures we are considering are such that the high-temperature approximation is very well justified (this approximation holds for $T > \Lambda = 500$). However, the physical origin of the result can be easily understood as follows: as seen in Fig. 4, the time t_{dec} we obtain from our computation is of the same order as the "collision" time $t_\Lambda = \Lambda^{-1} \simeq 2 \times 10^{-3}$ (remember that for zero temperature we obtained $t_{\text{dec}} \simeq 10^{-3}$). This is an extremely short time and on this scale the nonstationary (transient) effects produced by the environment are very important. Therefore, it is incorrect to assume that the diffusion coefficient is a constant given by $D = 2\gamma_0 k_B T$ since this is only the asymptotic value reached after a few times t_Λ. Thus, as the diffusion vanishes initially, decoherence must occur slower than predicted by (44). In fact, the rate (44) can only be a reasonable approximation provided that the predicted decoherence time t_{dec} is much larger than the collision time t_λ. The high-temperature approximation cannot be trusted on time scales smaller than $\hbar / k_B T$, since they correspond to energies larger than $k_B T$ which are out of the range of guaranteed validity of (42).

To test the validity of approximation (42) parameters should be chosen such that the decoherence rate is reduced. A way to achieve this is by decreasing the strength of the coupling γ_0. For this reason we studied the highly underdamped case $\gamma_0 = 0.001$. The results are shown in Fig. 6 where curve (i) represents the numerical results for A_{int} and curve (ii) the approximation (42). The two curves are almost identical for initial times and differences arise only when dynamical effects become important [as expected, since (42) is supposedly good only for times shorter than the dynamical time]. The good agreement between the approximation for the decoherence rate and the numerical results is well illustrated in Fig. 7 where curve (i) corresponds to the numerical results and curve (ii) to the approximation (44). The coincidence is rather remarkable and the difference is just as intuitively expected since we know that approximation (44) overestimates the rate at high temperatures (when

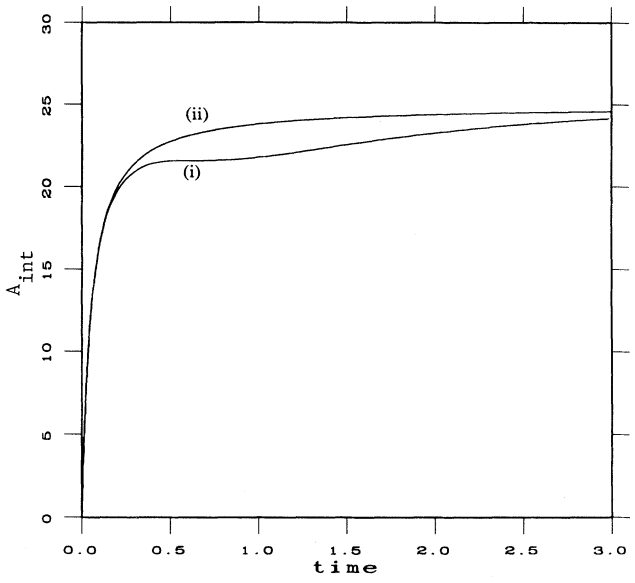

FIG. 6. The evolution of $A_{\rm int}$ in an extremely weakly damped case ($\gamma_0=0.0001$). We only display the curves corresponding to the initial condition A with a temperature $T_3=25\,000$. In this case decoherence takes place in a time scale that is larger than the collision time but still smaller than any dynamical time scale. Curve (*i*) corresponds to the numerical results and curve (*ii*) to the high-temperature approximation given by Eq. (38). In this case the accuracy of the approximation is excellent.

the decoherence time becomes comparable with the collision time) and underestimates it at low temperatures [where the rate predicted by (44) vanishes].

C. Supra-Ohmic environment

We will now study an environment that corresponds to $n=3$ in (5). This is a prototypical example of a supra-Ohmic environment used to describe various physical situations. It is possible to show that the effect of the interaction between a charged particle and its own electromagnetic field can be modeled by such an environment [22]. The interaction between a defect and phonons in a metal can be modeled by the $n=3$ environment and also by one with $n=5$ depending on the symmetry of the coupling [20,21].

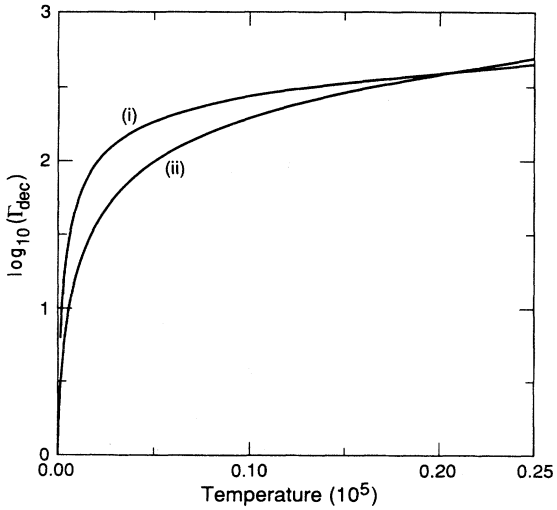

FIG. 7. The agreement between the decoherence rate calculated from our numerical results [curve (*i*)] and the one corresponding to the high-temperature approximation [curve (*ii*)] is remarkable in the regime of very weak damping ($\gamma_0=0.0001$).

The techniques we will use here are identical to the ones already described. As before, the local approximation can help us to get a flavor of the effect of the environment. It is easy to show that, in the limit $\Lambda\to\infty$, we can write

$$\int_0^s \eta(s-s')u(s')=\frac{2\gamma_0}{\Lambda^2}\{[\ddot{\delta}(0)u(s)+\delta(0)\ddot{u}(s) -\ddot{\delta}(s)u(0)-\dot{\delta}(s)\dot{u}(0) -\delta(s)\ddot{u}(0)]-\tfrac{1}{2}\ddot{u}(s)\}\ , \tag{48}$$

where we are using $\delta(s)=\Lambda\pi^{-1/2}\exp(-\Lambda^2 s^2)$ as the representation for the δ function. With the above equation in hand, we can see the effects introduced by the environment in Eq. (15). The first term on the right-hand side of (48) generates an infinite frequency renormalization $\Delta\omega^2=-8\gamma_0\Lambda\pi^{-1/2}$ which is of the same order as the one produced by the Ohmic environment. The second term produces an infinitesimal mass renormalization and the next three are "kick" terms [in the $\Lambda\to\infty$ limit the only important one is the one proportional to $u(0)$]. Finally, the last is a third derivative term but its effect is damped by a factor of Λ^{-2} and can be neglected in the local limit. Therefore, in the above approximation the equation for the functions $u_{1,2}$ is that of a free harmonic oscillator *without* dissipation and the coefficients $b_k(t)$ are given by (46) with $\gamma_0=0$. The fact that, in the long-time limit, there are no dissipative effects associated with this supra-Ohmic environment has been remarked on in Ref. [19] and can be understood as a consequence of the weakness of the spectral density in the infrared sector. In our numerical calculations, we solved Eq. (15) and compared the results with the local approximation finding a very good agreement for times of the order of $100\Lambda^{-1}$. The coefficients a_{ij} that determine the diffusion effects cannot be written in closed form (they can be expressed as integrals over simple functions). However, one expects that in accordance with the nonexistence of strong dissipative effects, the diffusion will also tend to vanish in the long-time regime. This expectation is, in fact, correct as was shown in Ref. [19] where the time dependence of the diffusion coefficient appearing in (37) was studied. In the long-time limit, the normal diffusion is very small and its effect becomes comparable to the anomalous diffusion.

In our numerical calculations we considered a system characterized by the same parameters we had in the Ohmic case: we used units in which $\Omega_{\rm ren}=1$, set the high-frequency cutoff to $\Lambda=500$, and analyzed the case $\gamma_0=0.3$. In Figs. 8(a) and 8(a') we have plotted the function $A_{\rm int}$ for the initial conditions A and A', respectively. Let us first analyze Fig. 8(a) where some very interesting effects can be seen. For the high-temperature case the

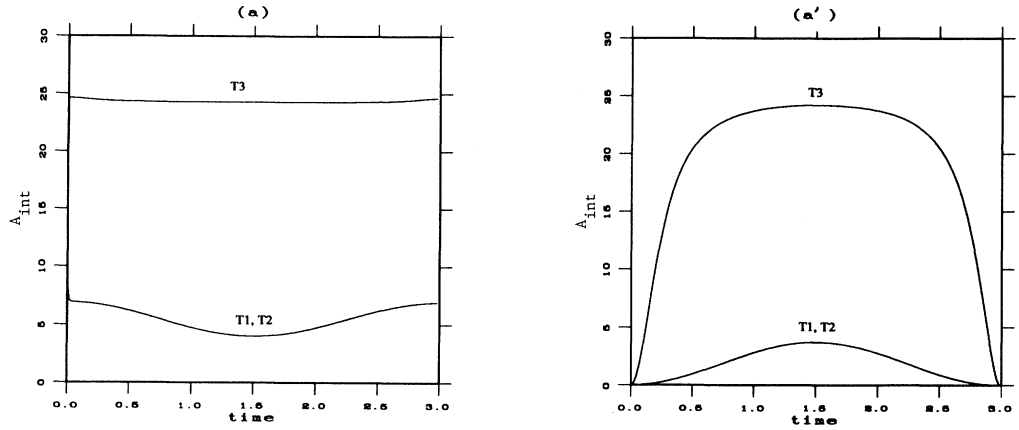

FIG. 8. The evolution of $A_{\rm int}$ for a harmonic oscillator in a supra-Ohmic environment at temperatures $T_1=0$, $T_2=10$, and $T_3=25\,000$. For the initial condition A (a) the system is sensitive to the initial transient that is strong enough to produce decoherence. In the stationary regime, the environment does not produce irreversible behavior and, after a small oscillation, the value of $A_{\rm int}$ returns to the one it had reached after the initial jolt. On the contrary, for condition A' the interaction is not effective initially since $L_0=0$. When the centers become spatially separated, the environment is no longer able to produce irreversible behavior and decoherence is not achieved in this case.

decoherence time $t_{\rm dec}$, is of the same order as that corresponding to the Ohmic environment. For lower temperatures, we observe that the maximum possible value of $A_{\rm int}=L_0^2/\delta^2+\delta^2P_0^2$ is never reached since the function grows very fast initially, reaches a value $A_{\rm int}(0^+)$, and then starts an oscillatory regime with a frequency that seems to coincide with the oscillator frequency. After the oscillator makes a complete turn, the value of $A_{\rm int}$ returns to $A_{\rm int}(0^+)$. The existence of oscillations in $A_{\rm int}$ is not surprising and can be shown to be an amplification of the effect we observed for the Ohmic environment in Fig. 3. It is associated with the anomalous diffusion which generates the second term on the right-hand side of (39). The sign of this term changes with time as the two packets rotate thus inducing the oscillations.

It is important to stress that, according to our previous discussion, one expects this environment to be unable to produce irreversible effects since in the long-time regime there is no dissipation nor a normal diffusion. However, in Fig. 8(a) we observe an irreversible loss of coherence that in the high-temperature case seems to be very important. In fact, even in the low-temperature regime there is an irreversible loss of coherence since, despite having a nonmonotonic behavior, $A_{\rm int}$ never goes back to zero but returns to $A_{\rm int}(0^+)$. This effect cannot be explained using the local approximation or the long-time values of the diffusion coefficients since it is entirely due to the short-time response of the environment. In fact, the irreversible loss of quantum coherence takes place on a time scale of the order of $\tau_\Lambda=\Lambda^{-1}$. As was noted in Ref. [19], the diffusion coefficient has a strong peak on a time scale of the order of τ_Λ and reaches a value that is universal and essentially fixed by the cutoff $h(t_\Lambda)=2\gamma_0\Lambda$. After this initial cutoff dominated regime, the diffusion coefficient evolves in an environment dependent way towards some asymptotic value. Our results show that for the supra-Ohmic environment all the decoherence is produced by this initial peak in diffusion. In contrast, for an Ohmic environment the effect of the initial peak in diffusion can be important but it is always followed by the effect produced by normal diffusion in the stationary regime (it is worth noticing that the effect of the initial jolt can be made arbitrarily small in the low damping limit, as illustrated by the second example discussed in Sec. III B, see Figs. 6 and 7). The above property of the supra-Ohmic environment allows us to present arguments against the physical relevance of the initial jolt. It can be argued that the transient behavior, which is caused by the initial peaks in the diffusion coefficients, is strongly related to the initial condition we used (no correlations between the system and the environment at the initial time). Initial correlations are likely to wash out the initial peaks in the diffusion coefficients. However, the physical irrelevance of the initial jolt is better illustrated in Fig. 8(a') where we observe that for the initial condition A' no irreversible loss of coherence is achieved. The initial jolt is completely innocuous and the reason for this is clear: the jolt becomes irrelevant because the initial condition A' is such that the interaction with the environment is initially very inefficient. The centers of the two wave packets have to become spatially separated but by the time this happens the environment is incapable of producing irreversible behavior.

IV. DISCUSSION

The purpose of this paper was to present a detailed study of the process of decoherence in an exactly solvable case—a double-slit inspired situation—where the state vector is initially a coherent superposition of two wave packets which are separately localized in both position and momentum and therefore can be regarded as poten-

tial candidates for the classical "points in the phase space." We have found that the rate of loss of quantum coherence between such minimum uncertainty states is indeed correlated with the spatial correlation between them and, as originally estimated in Ref. [15], that the characteristic decoherence time scale is quite well approximated by the simple formula (2) whenever the high-temperature approximation is valid. Moreover, even outside the range of validity of the high-temperature approximation a natural extrapolation of (2) given by (42) applies.

The preferred role of the observable which couples the system to the environment is apparent in our results. In particular, the rate of coherence loss is much faster when the wave packets are initially separated in position. Moreover, a superposition of two wave packets which differ in momentum, but have identical positions, decoheres solely because the initial difference in momentum translates into a subsequent difference of positions, which allows for the "monitoring by the environment," which, in turn, leads to decoherence. In fact, (39) tells us that $A_{\rm int}$, which is a measure of the effectiveness of decoherence, does not grow when the centers of the two wave packets have the same position [for weakly damped systems $\kappa_p \propto x_c(t)$].

The goal of these considerations is a better understanding of the mechanisms which precipitate the transition from quantum to classical. In this context the important characteristic of the decoherence process we have studied is not the fact that the off-diagonal terms of the density matrix are negligible in *some* basis—there is always a basis in which they are exactly zero, simply because the density matrix is a Hermitian operator, and, therefore, will be diagonalized by its eigenstates. Rather, one should focus on the invariance of the basis which will always nearly diagonalize the reduced density matrix after the decoherence time, regardless of what was its initial form. Thus, the emergence of classical states of the systems (which are localized in both position and momentum) can be seen as a consequence of the ability of the decoherence process to differentiate between the rates with which different pure states in the Hilbert states decay into mixtures.

While we have focused on a rather limited set of initial conditions (superpositions of Gaussians) one could argue that our results strongly suggest that the preferred basis must consist of states very similar (if not necessarily identical) to the localized Gaussian wave packets. This is simply because minimum uncertainty wave packets constitute a basis in the Hilbert space. Therefore, any state can be expressed in terms of their superpositions. But any superposition can be regarded as a sum over pairs of such Gaussians. Moreover, any superposition which is substantially nonlocal in either x or p will decohere on a time scale which can be deduced from the above considerations (and which is considerably shorter than the time scale over which individual localized Gaussians decohere). Therefore, it follows that the set of preferred "pointer" states singled out by the evolution of open systems has an appealing feature of being close to what one would want to associate with points in the classical phase space.

Given that we have apparently extracted from the quantum substrate some of the elements useful in establishing the connection between the quantum and the classical, it is now useful to look again at our assumptions. The model we have used is clearly selected according to the criteria of calculational convenience rather than because it is realistic. One can nevertheless expect that even in the situations where the linearity of the model is an approximate, rather than exact, feature, the rapid rate of decoherence (which for macroscopic systems at "room temperatures" occurs on a time scale very much more rapid than the dynamics) will force any initial state into a mixture of localized wave packets. Thus, in order to investigate the process of decoherence experimentally in the transition region where the ability of the environment to enforce the environment-induced superselection is noticeable but not overwhelming, one must consider either extremely well-isolated classical systems (such as a cryogenic Weber bar) or, quantum systems prepared in very nonclassical states.

Initial conditions used in the model were also idealized. Nevertheless, one could argue that the only truly unphysical consequence of the assumed initial product structure of the joint state of the system and of the environment is the initial non-Markovian evolution on time scales of the order of the upper frequency cutoff. We illustrated the unphysical nature of the effect produced by the initial transient (that produces a strong initial peak in the diffusion coefficient) by using a supra-Ohmic environment where the effect of the initial diffusion peak can be made innocuous by choosing appropriate initial conditions [26]. Moreover, while the dependence of the process on the spectral density of the environment leads to interesting questions about the nature of decoherence and its relation to the definition of what is "the system" at sufficiently low temperatures (that is, how to treat vacuum modes which can be adiabatically dragged with the observables of interest, and, therefore, should not be regarded as the part of the decoherence-causing environment, as appears to be the case in the supra-Ohmic example described above) it is unlikely to make a major difference in the context usually regarded as classical. And, last but not least, the nature of the interaction Hamiltonian which "decided" the form of the preferred observable, the one which decoheres most rapidly, is again motivated by physics: Interaction potentials usually depend on position [7,9,15]. Therefore, choosing an $H_{\rm int}$ which commutes with x was rather natural. Moreover, coupling terms higher order in x would have changed the nature of the diffusion process, but not the preferred observable.

Thus, while our model was rather special, one can hope that the results we have obtained should be qualitatively applicable to a broader range of conditions and can be a basis for discussion of the transition from quantum to classical in a much more general context. In this paper we have not compared our approach with the "consistent histories" formulation of Griffiths, Omnès, and Gell-Mann and Hartle (we refer the reader to Ref. [27] for an introduction to recent developments). There, the focus of attention is on the additivity of probabilities for

histories—time-ordered sequences of events represented by projection operators. The corresponding "consistency conditions" which assure such additivity are rather easy to satisfy allowing for many sets of consistent histories most of which are flagrantly nonclassical [27,13,29]. Thus, additional constraints on the allowed histories have to be introduced to define the quasiclassical domain. Such conditions have not yet been proposed in a manner which would allow a rigorous investigation. On the other hand, environment-induced superselection is expected to yield consistent histories whenever the projection operator employed to represent events are constructed out of the pointer eigenspaces [13,29]: successful decoherence is then expected to be a guarantee of consistency. These and other conceptual connections between the two formalisms, which were discussed in Ref. [13], will be analyzed elsewhere [29]. A first analysis of the consistent histories approach to the Caldeira-Leggett model (focusing on a single Gaussian initial state and for the high-temperature regime) can be found in Ref. [28].

[1] A. Aspect, P. Grangier, and G. Roger, Phys. Rev. Lett. **47**, 91 (1982); A. Aspect, J. Dalibard, and G. Roger, *ibid.* **49**, 1804 (1982).
[2] B. Yurke and D. Stoler, Phys. Rev. Lett. **57**, 13 (1986).
[3] C. Tesche, Phys. Rev. Lett. **64**, 2358 (1990).
[4] S. Habib and R. Laflamme, Phys. Rev. D **42**, 4056 (1990); J. P. Paz and S. Sinha, *ibid.* **44**, 1038 (1991); **45**, 2823 (1992), and references therein.
[5] C. M. Caves, K. S. Thorne, R. W. P. Drever, V. D. Sandberg, and M. Zimmermann, Rev. Mod. Phys. **52**, 341 (1980).
[6] W. M. Itano, D. J. Heinzen, J. J. Bollinger, and D. J. Wineland, Phys. Rev. A **41**, 2295 (1990).
[7] W. H. Zurek, Phys. Today **44**, 36 (1991).
[8] W. H. Zurek, Phys. Rev. D **24**, 1516 (1981).
[9] W. H. Zurek, Phys. Rev. D **26**, 1862 (1982).
[10] E. Joos and H. D. Zeh, Z. Phys. B **59**, 223 (1985).
[11] H. D. Zeh, *The Physical Basis of the Direction of Time* (Springer-Verlag, New York, 1989), and references therein.
[12] A. O. Caldeira and A. J. Leggett, Physica A **121**, 587 (1983), and see therein for references to earlier work.
[13] W. H. Zurek, in *The Physics of Time Asymmetry,* edited by J. J. Halliwell, J. Perez-Mercader, and W. H. Zurek (Cambridge University Press, Cambridge, England, in press).
[14] W. H. Zurek, S. Habib, and J. P. Paz, "Coherent states via decoherence," Los Alamos Report No. LA-UR-92-1642, 1992 (unpublished).
[15] W. H. Zurek, in *Frontiers of Nonequilibrium Statistical Physics,* edited by G. T. Moore and M. O. Scully (Plenum, New York, 1986).
[16] L. S. Bartell, Phys. Rev. D **21**, 1698 (1980).
[17] W. G. Unruh and W. H. Zurek, Phys. Rev. D **40**, 1071 (1989).
[18] F. Haake and R. Reiboldt, Phys. Rev. A **32**, 2462 (1982).
[19] B.-L. Hu, J. P. Paz, and Y. Zhang, Phys. Rev. D **45**, 2843 (1992).
[20] H. Grabert, P. Schramm, and G.-L. Ingold, Phys. Rep. **168**, 115 (1988).
[21] A. J. Leggett, S. Chakravarty, A. T. Dorsey, M. P. A. Fisher, A. Garg, and W. Zwerger, Rev. Mod. Phys. **59**, 1 (1987).
[22] P. M. V. B. Barone and A. O. Caldeira, Phys. Rev. A **43**, 57 (1991).
[23] E. P. Wigner, Phys. Rev. **40**, 749 (1932). For an excellent review, see M. Hillery, R. F. O'Connell, M. O. Scully, and E. P. Wigner, Phys. Rep. **106**, 121 (1984).
[24] A. O. Caldeira and A. J. Leggett, Phys. Rev. A **31**, 1059 (1985).
[25] V. Ambegaokar, Ber Bunsenges. Phys. Chem. **95**, 400 (1991).
[26] J. P. Paz, in *The Physics of Time Asymmetry* [13].
[27] R. Omnès, Rev. Mod. Phys. **64**, 339 (1992); M. Gell-Mann and J. B. Hartle, in *Complexity, Entropy, and the Physics of Information,* edited by W. H. Zurek (Addison-Wesley, Reading, PA, 1990).
[28] J. P. Paz and W. H. Zurek, "Environment induced superselection and the consistent histories approach to decoherence," Los Alamos Report No. LA-UR-92-878, 1992 (unpublished).
[29] H. F. Dowker and J. J. Halliwell, Phys. Rev. D **46**, 1580 (1992).